

Geant4 simulation strategy and event reconstruction for HEPD-02 detector onboard the CSES-02 Satellite.

Andrea Contin,^{a,b} Andrea Di Luca,^{c,d} Francesco Maria Follega,^{d,e} Roberto Iuppa,^{d,e} Mauro Lolli,^b Alberto Oliva,^b Federico Palmonari,^b Michele Pozzato,^b Ester Ricci^{d,e} and Zouleikha Sahnoun^{a,b,*} for the CSES-Limadou Collaboration

^aUniversity of Bologna, V.le C. Berti Pichat 6/2, I-40127 Bologna, Italy

^bIstituto Nazionale di Fisica Nucleare, Sezione di Bologna, V.le C. Berti Pichat 6/2, I-40127 Bologna, Italy

^cFondazione Bruno Kessler, V. Sommarive 18, I-38123 Povo (Trento), Italy

^dTrento Institute for Fundamental Physics and Applications, V. Sommarive 14, I-38123 Povo (Trento), Italy

^eUniversity of Trento, V. Sommarive 14, I-38123 Povo (Trento), Italy

E-mail: zouleikha.sahnoun@bo.infn.it

The High Energy Particle Detector (HEPD-02) is one of the scientific payloads of the China Seismo-Electromagnetic Satellite (CSES-02) aimed to measure particle precipitation due to short-time perturbations in the radiation belts caused by solar and terrestrial phenomena. Developed by the CSES-Limadou collaboration, HEPD-02 will measure particle flux and energy spectrum in a wide range of energies and was designed to improve the performance of the 1st generation detector. We report on the Geant4 Monte Carlo simulation developed to study the response of the new detector. In addition to the detailed simulation, a parametric approach was also developed in order to reduce simulation time without losing performance or precision. An event reconstruction software is used to estimate the arrival direction, energy, and identity of the incoming particles. Moreover, specifically designed neural networks are trained using the ADC signals from the calorimeter and the particle impact position and direction to better reconstruct the deposited energy, correcting for the energy lost in the inert materials obtained from simulation.

38th International Cosmic Ray Conference (ICRC2023)
26 July - 3 August, 2023
Nagoya, Japan



*Speaker

1. Introduction

The China Seismo-Electromagnetic Satellite (CSES) is a series of Chinese-Italian space missions dedicated to monitoring of the near-Earth environment [1, 2]. Their main goal is to study the possible correlation of electromagnetic field, plasma, and particle flux variations with the occurrence of strong seismic events. They also have the capability to study perturbations due to solar and cosmic phenomena [3–5]. The High-Energy Particle Detector (HEPD) developed by the Italian CSES-Limadou collaboration, is one of the scientific instruments on board the CSES mission. The first satellite has been flying since February 2018; the second one, CSES-02, which will carry HEPD-02, is expected to be put into a sun-synchronous orbit in early 2024. HEPD-02 is designed to identify particles in a wide range of energies: from 3 to 100 MeV for electrons, 30 to 200 MeV/n for protons and light nuclei, and to measure their flux and precipitation ("particle burst") from the inner Van Allen belt due to cosmic or terrestrial perturbations. A brief description of the instrument is given in section 2. Detector performance was evaluated using a Geant4-based Monte Carlo simulation assuming an isotropic incoming flux of electrons, protons, and alpha particles on top of the instrument, showing the design meets the mission's scientific requirements [6]. In the following, we report on the Monte Carlo simulation developed for the HEPD-02 detector and on the reconstruction strategy. We describe a parametric approach based on 2D and 3D maps of the light output versus hit position for each sub-detector, allowing us to save on full event simulation time. Preliminary results on the tuning of the detector with the use of experimental data are also presented.

2. The High Energy Particle Detector

The High Energy Particle Detector (HEPD-02) is composed of several detectors as shown in Fig. 1. It consists of:

- a first trigger plane (**TR1**) made up by 5 2 mm plastic scintillator counters of $32 \times 154 \text{ mm}^2$.
- an incident particle angle detector **DD** ("tracker"), $150 \times 150 \text{ mm}^2$ made of five standalone tracking modules, each composed of three sensitive planes.
- a second trigger plane (**TR2**), orthogonal to TR1, composed of four 8 mm scintillators with dimensions $36 \times 150 \text{ mm}^2$.
- an energy detector **ED** made of a tower of 12 10 mm plastic scintillators (RAN1, ..., RAN12), $150 \times 150 \text{ mm}^2$, and two orthogonal layers of three 25 mm LYSO crystals, $50 \times 150 \text{ mm}^2$.
- five plastic scintillator panels 8 mm thick, covering the sides and the bottom of the calorimeter composing the containment detector (**CD**).

All the scintillators are wrapped in aluminized mylar and readout by 2 Hamamatsu R9880U-210 photomultiplier tubes (PMT) at opposite ends. Details on the detector design can be found in [6, 7].

HEPD-02 is able to detect particles on an event-by-event basis. For each individual particle, the energy is measured and the angle between its direction and the magnetic field lines (pitch angle) is determined.

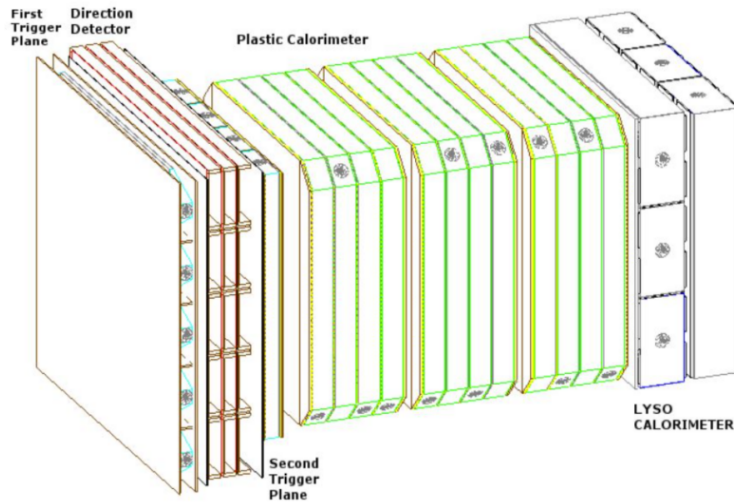


Figure 1: HEPD-02 detector layout. The containment panels are not shown.

3. Simulation

A Monte Carlo simulation has been developed using the Geant4 toolkit [8], in order to study the response of the detector to protons, electrons, and light nuclei. The full simulation takes a set of GDML files exported from the TCAD model of the detector. It includes all the sensitive detectors (TR1, DD, TR2, ED, and CD), the inert materials, as well as the mechanical structure and electronic box. The simulation is implemented taking into account the optical properties of the materials, such as the light emission spectra of plastic scintillators (EJ-200) and crystals (LYSO), and the photomultiplier's photon-to-electron conversion efficiency. The light absorption coefficients and the reflectivity of the wrapping material are left as adjustable parameters used to tune the simulation to the experimental data.

In the simulation, when a particle passes through the detector, its position, direction, and energy release in each sensitive detector subsystem are recorded. The energy released within the inert materials is also kept for reconstruction purposes. When running in full optical mode, i.e., with the emission and propagation of scintillation photons, the number of photo-electrons collected by each PMT is also recorded. Several experimental tests were carried out in the laboratory with cosmic muons in order to check the efficiency and uniformity of the single counters. These tests were also very useful for a first tuning of the simulation parameters. As an example, in Fig.2 a comparison of the most probable number of photo-electrons registered by a single counter of the second trigger plane (TR2) with that obtained from the tuned simulation as a function of the longitudinal impact position of the cosmic muons is shown. The same comparison and tuning were made for all the HEPD-02 sub-detectors.

3.1 Photo-electron sampling

Running simulation with optical photons is very time-consuming and CPU-intensive, so a parametric approach has been developed in order to speed up the digitization process. It consists

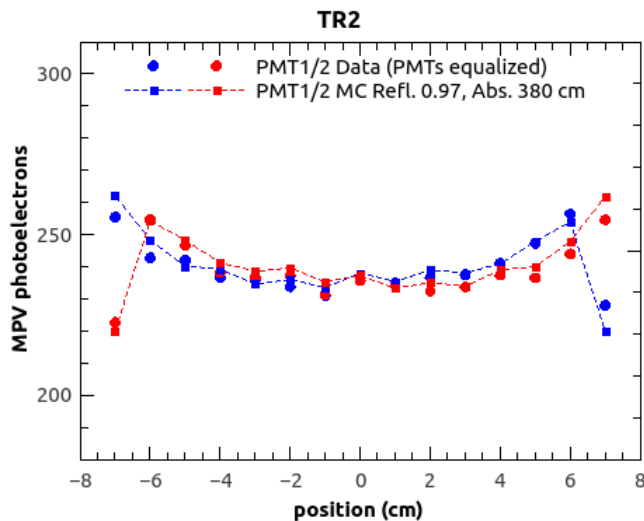


Figure 2: Comparison of the most probable number of photo-electrons obtained from simulation with experimental data as a function of longitudinal position for a TR2 trigger counter.

of constructing 2D/3D maps of the average number of photo-electrons relative to the center of a specific counter generated from a certain energy deposit as a function of the impact position. These maps, combined with the distribution of the mean photo-electron number at the center of the counter as a function of the deposited energy and the corresponding ADC signal obtained from the calibration curves of the PMT readout system, can be used for fast digitization. An example 2D map is shown in Fig.3, for photo-electrons collected by one of the phototubes of the TR2 paddle, as a function of the impact position (x,y) . As the second phototube is on the opposite side of the TR2 bar, the map obtained is perfectly symmetrical with respect to the centre. In Fig.4, the number of photo-electrons recorded as a function of the energy deposited in the center of the counter is given. With these two parametrizations, for a given energy release in the detector, one can sample from a Poisson distribution the number of photo-electrons collected by the PMTs for any primary impact position on the counter and the related ADC signal.

4. Event Reconstruction

To reconstruct events a software was developed to estimate the arrival direction, energy, and identity of the incoming particles. It is based on the clustering of pixels in each tracking module using a DBscan [9] algorithm and then a Hough Transform [10] to reconstruct the tracks. Finally, a 3D linear fit of triplets obtained from the three sensitive planes makes it possible to reconstruct the direction of the particles.

Dedicated neural networks are designed using PyTorch [11] and trained using the signals recorded in all the sub-detectors from Monte Carlo digitisation or data acquisitions. A deep learning algorithm for regression ¹ is used to reconstruct the initial energy. It consists of a meta-estimator that fits an optimized number of decision trees, each on different subsamples of the full dataset, and then

¹<https://pytorch.org/docs/stable/generated/torch.nn.L1Loss.html>

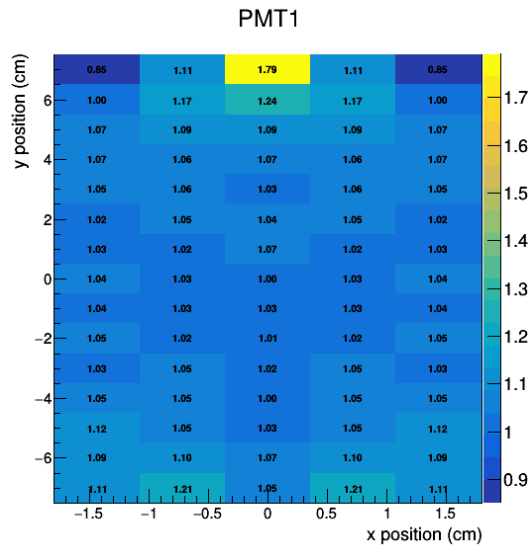


Figure 3: Map of the relative number of photo-electrons with respect to the center of the counter for different interaction areas as seen by the PMT in the positive Y position.

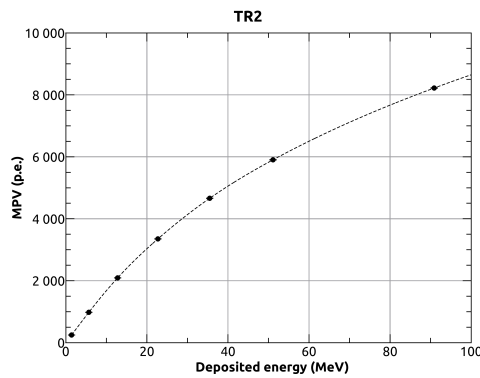


Figure 4: The number of photo-electrons collected as a function of the energy deposited in the center of a TR2 counter.

uses the average to prevent overfitting and improve performance. It is trained using the ADC signals from the calorimeter and the particle impact position and direction to better reconstruct the deposited energy, correcting for the energy lost in the inert materials, such as covers or mechanical structure, obtained from simulation. In Fig.5, are shown the reconstructed energy versus the simulated one from an independent Monte Carlo proton sample (left) and the estimated resolution (right). The simulation shows that with the adopted design and selection criteria, the uncertainty on reconstructed energy is less than 10% for kinetic energies > 30 MeV.

To identify the type of particle a classifier algorithm ² was trained to discriminate between electrons and protons, and separate between electrons, protons and alpha particles. In Fig.6, is shown an example of the achievable discrimination between electrons, protons, and He nuclei. In this case the algorithm exploits the different charge deposits of the various particles. Preliminary

²<https://pytorch.org/docs/stable/generated/torch.nn.BCELoss.html>

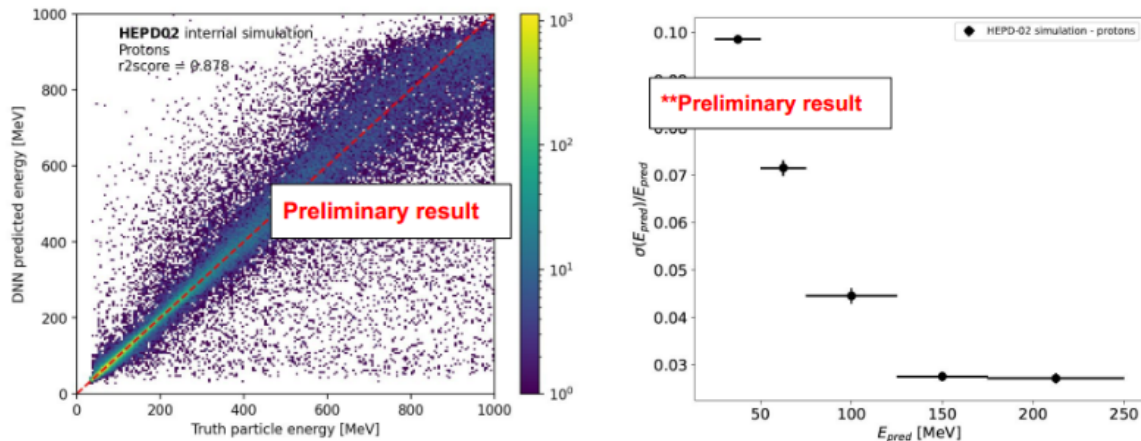


Figure 5: The energy reconstructed from the Neural network and its resolution as a function of the true simulate energy for a sample of protons incident on HEPD-02.

results shows that the particle identification accuracy can be better than 95%.

5. Conclusions

In this paper, the results of the simulation of the HEPD-02 detector carried out with the Geant4 tool have been reported. The digitization procedure and the parametric approach implemented to speed up the simulation were also presented. Preliminary results on the event reconstruction algorithms using fully connected neural networks from an isotropic incoming flux of electrons, protons, and alpha particles on top of the instrument allowed to derive the performances of the detector, showing performances that meet expectations. The HEPD-02 device is being extensively tested under electron and ion beams at the beam test facilities. Analysis of the data obtained from these tests will allow better tuning of the simulation parameters and to fully test and further develop the parameterised digitisation.

Acknowledgments

This work was supported by the Italian Space Agency in the framework of the agreement between ASI and INFN “Accordo Attuativo 2020-32.HH.0 Limadou Scienza+”.

References

- [1] X. Shen *et al.*, *Sci. China Tech. Sci.* **61** (2018) 634.
- [2] P. Picozza *et al.*, *Ap. J. Supp. Ser.* **243** (2019) 16.
- [3] F. Palma *et al.*, *Appl. Sci.* **11** (2021) 5680.
- [4] M. Martucci *et al.*, *Space Weather* **21** (2023) 1.

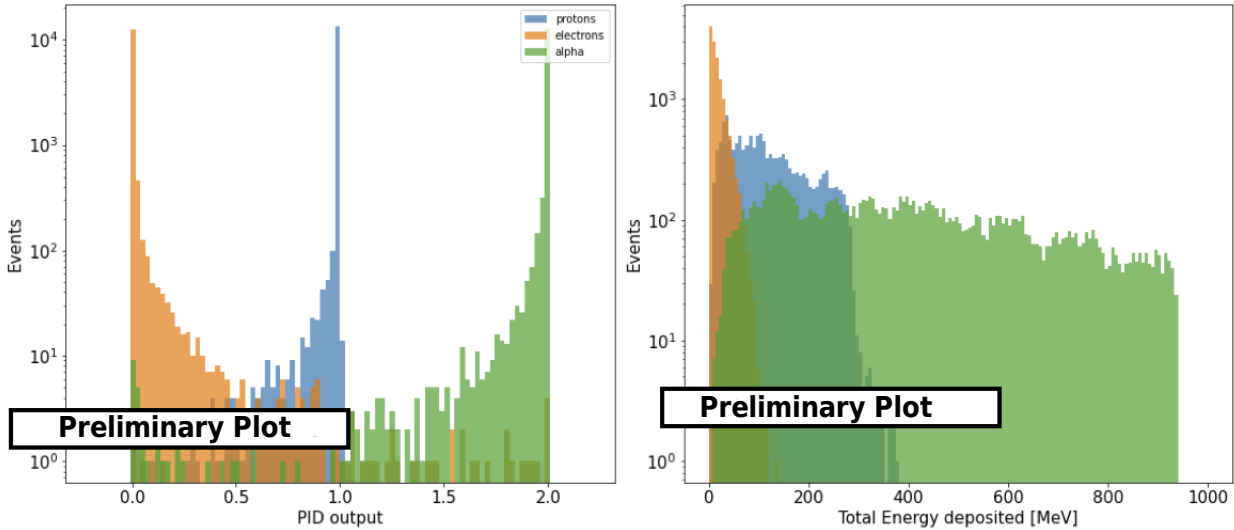


Figure 6: On the left the distribution of the PID output for electrons (orange), protons (blue) and alpha (green). On the right the distribution of the total energy deposited for the same particles.

- [5] M. Martucci *et al.*, *Astroph. J. Lett.* **945** (2023) L39.
- [6] C. De Santis *et al.*, *Proc. of the 37th Int. Cosmic Ray Conf.* (2021) 058.
- [7] A. Ambrosi *et al.*, Internal Report, RPT-LIM2-004-2.
- [8] S. Agostinelli *et al.*, *Nucl. Instrum. Methods Phys. Res. A* **506** (2003) 250.
- [9] M. Ester *et al.*, *Proc. of the 2nd Int. Conf. on Knowledge Discovery and Data Mining* (1996) 226–231.
- [10] R. O. Duda and P. E. Hart, *Comm. ACM*, **15** (1972) 11–15.
- [11] A. Paszke *et al.*, *Adv. in Neural Information Processing Systems* **32** (2019).

Full Authors List: CSES-LIMADOU Collaboration

S. Bartocci¹, R. Battiston^{2,3}, F. Benotto⁴, S. Beolé^{4,5}, W.J. Burger^{3,6}, D. Campana⁷, G. Castellini⁸, P. Cipollone¹, S. Coli⁴, L. Conti^{1,9}, A. Contin^{10,11}, M. Cristoforetti¹², L. De Cilladi^{4,5}, C. De Donato¹, C. De Santis¹, F.M. Follega^{2,3}, G. Gebbia^{2,3}, R. Iuppa^{2,3}, M. Lolli¹¹, N. Marcelli^{1,13}, M. Martucci^{1,13}, G. Masciantonio¹, M. Mergé^{1,†}, M. Mese^{7,14}, C. Neubuser³, F. Nozzoli³, A. Oliva¹¹, G. Osteria⁷, L. Pacini¹⁵, F. Palma^{1,†}, F. Palmonari^{10,11}, A. Parmentier¹, F. Perfetto⁷, P. Picozza^{1,13}, M. Piersanti¹⁶, M. Pozzato¹¹, E. Ricci^{2,3}, M. Ricci¹⁷, S.B. Ricciarini⁸, Z. Sahnoun^{10,11}, V. Scotti^{7,14}, A. Sotgiu^{1,13}, R. Sparvoli^{1,13}, V. Vitale¹, S. Zoffoli¹⁸ and P. Zuccon^{2,3}

¹ INFN-Sezione di Roma “Tor Vergata”, V. della Ricerca Scientifica 1, I-00133 Rome, Italy;

² University of Trento, V. Sommarive 14, I-38123 Povo (Trento), Italy;

³ INFN-TIFPA, V. Sommarive 14, I-38123 Povo (Trento), Italy;

⁴ INFN-Sezione di Torino, Via P. Giuria 1, I-10125 Torino, Italy;

⁵ University of Torino, Via P. Giuria 1, I-10125 Torino, Italy;

⁶ Centro Fermi, V. Panisperna 89a, I-00184 Rome, Italy;

⁷ INFN-Sezione di Napoli, V. Cintia, I-80126 Naples, Italy;

⁸ IFAC-CNR, V. Madonna del Piano 10, I-50019 Sesto Fiorentino (Florence), Italy;

⁹ Uninettuno University, C.so V. Emanuele II 39, I-00186 Rome, Italy;

¹⁰ University of Bologna, V.le C. Berti Pichat 6/2, I-40127 Bologna, Italy;

¹¹ INFN-Sezione di Bologna, V.le C. Berti Pichat 6/2, I-40127 Bologna, Italy;

¹² Fondazione Bruno Kessler, V. Sommarive 18, I-38123 Povo (Trento), Italy;

¹³ University of Rome “Tor Vergata”, V. della Ricerca Scientifica 1, I-00133 Rome, Italy;

¹⁴ University of Naples “Federico II”, V. Cintia 21, I-80126 Naples, Italy;

¹⁵ INFN-Sezione di Firenze, V. Sansone 1, I-50019 Sesto Fiorentino (Florence), Italy;

¹⁶ INAF-IAPS, V. Fosso del Cavaliere 100, I-00133 Rome, Italy;

¹⁷ INFN-LNF, V. E. Fermi 54, I-00044 Frascati (Rome), Italy;

¹⁸ Italian Space Agency, V. del Politecnico, I-00133 Rome, Italy;

† At ASI Space Science Data Center (SSDC) also, V. del Politecnico, I-00133 Rome, Italy.